J Solid State Electrochem (2007) 11:1567–1573
DOI 10.1007/s10008-007-0360-y

ORIGINAL PAPER

In situ FTIRS studies of the electrocatalytic oxidation of ethanol on Pt alloy electrodes

D. M. dos Anjos · F. Hahn · J.-M. Léger · K. B. Kokoh · G. Tremiliosi-Filho

Received: 28 February 2007 / Revised: 16 May 2007 / Accepted: 16 May 2007 / Published online: 13 July 2007

Abstract Ethanol oxidation on Pt–Os and Pt–Ru–Os alloy electrodes was investigated by electrochemical and spectroelectrochemical techniques. Cyclic voltammetry and chronoamperometric results showed that the Pt–Os alloy has the highest current density at lower potentials. Linear CO_{ads}, acetic acid, acetaldehyde, and CO_2 were identified as reaction intermediates and/or products by single potential alteration infrared reflectance spectroscopy and subtractively normalized interfacial Fourier transform infrared reflectance spectroscopy techniques. The in situ Fourier transform infrared spectroscopy results showed that the electrooxidative adsorption of ethanol was dissociative providing CO_{ads} at low potentials.

Keywords Ethanol electrooxidation · Pt–Os · Pt–Ru–Os · Infrared reflectance spectroscopy

Introduction

Several investigations have been carried out particularly during the last two decades on the electrooxidation of ethanol [1–5]. Ethanol is a molecule of considerable interest because of its importance and potential use as renewable fuel (obtained from sugar cane for example) for fuel cell applications [4, 5]. Among the various alcohols that can be considered as alternative fuels, ethanol is the most promising. It is a safe molecule in comparison to methanol, is liquid, and is easier to be stored and handled when compared to hydrogen. Moreover, ethanol has a high theoretical mass energy (6.1 kWh kg^{-1} for methanol vs 8.0 kWh kg^{-1} for ethanol) [6, 7]. The main disadvantage of ethanol comes from its molecular structure with a carbon containing a primary alcohol function and a second one as a methyl group. This molecular configuration induces a hard conversion of ethanol into carbon dioxide because of the difficulty to carry out the C–C bond cleavage and the complete oxidation of the methyl group using Pt as an electrocatalyst.

Although ethanol oxidation could not be complete providing 12 electrons per molecule, many reports showed that the main reaction products were acetaldehyde and acetic acid producing two to four electrons per molecule, which is so far from the maximum theoretical yield, but it is acceptable for application in low power sources such as portable electronic devices [8–10], even if the main objective is to find a catalyst that is able to oxidize ethanol to more than a four-electron conversion.

Nevertheless, lots of studies on the electrooxidation of ethanol devoted mainly to identify the adsorbed intermediates showed the presence of carbon monoxide species strongly adsorbed at the electrode surface. Identification of intermediates and final products, from the electrochemical oxidation of ethanol, was provided by many authors with the use of differential electrochemical mass spectrometry (DEMS) and in situ Fourier transform infrared spectroscopy (FTIRS) [11–14]. DEMS experiments identified acetaldehyde and CO_2 as primary reaction products, and using

Dedicated to our friend Professor Francisco Carlos Nart (in memorium), IQSC-USP, Brazil.

D. M. dos Anjos · G. Tremiliosi-Filho (✉)
Instituto de Química de São Carlos, Universidade de São Paulo,
Caixa Postal 780, 13560-970 São Carlos, SP, Brazil
e-mail: germano@iqsc.usp.br

D. M. dos Anjos · F. Hahn · J.-M. Léger · K. B. Kokoh
Equipe Electrocatalyse, UMR 6503, CNRS,
Université de Poitiers,
40, Avenue du Recteur Pineau,
86022 Poitiers Cedex, France

isotope-labeling strategies, these studies showed that acetaldehyde is formed by cleavage of the C–H bond in the α-carbon and the O–H bond in the hydroxyl group, while CO_2 is formed through a multistep pathway involving a strongly bonded intermediate. These experiments also indicated that the carbon atom in the CO_2 molecule is originated either from the methyl group or from the alcohol group of ethanol. Elsewhere, methane and ethane were also detected as desorption products at low potentials, probably issued from the methyl radical formed just after the C–C bond cleavage [13, 14]. FTIRS experiments showed that adsorbed carbon monoxide is an important intermediate strongly adsorbed at the Pt surface [15–29]. To enhance ethanol electrocatalytic oxidation and to decrease the poisoning of the catalyst, modification in the catalyst composition becomes necessary. To achieve this purpose, modifications of the electrode surface are usually suggested by adding other transition metal (M) such as Ru, Sn, Mo, Rh, Os, etc. to Pt [30–36]. It is well known that the presence of these metals as Pt–M alloys or Pt–M bimetallic catalysts improve the catalytic effect of platinum because of the bifunctional mechanism. In this mechanism, the partially oxidized M species supplies the oxygenated species for improving the oxidation of the adsorbates. A catalytic effect can also be explained by the ligand effect where the metal M atoms close to Pt are expected to influence the density of electronic states of Pt leading to the weakening of the Pt–CO bond [36–39]. The Pt–Ru system represents a promising alternative catalyst for ethanol oxidation. Early investigations carried out by in situ FTIR spectroscopy have shown that this catalyst could break the ethanol C–C bond at low potentials [40]. Later studies [41] have shown that Ru is not selective for CO_2 production. However, bands corresponding to the formation of CO_2, acetaldehyde, and acetic acid were present for all the compositions of the catalysts studied, and their relative intensities were clearly dependent on Ru composition and the applied potential. Fujiwara et al. [42] used the DEMS technique to study the reactivity and selectivity of ethanol oxidation on Pt–Ru electrodes. They found that Ru acts as an oxygen supplier at low potentials but also inhibits the ethanol adsorption during a subsequent oxidation on Ru sites. Wieckowski and et al. [31, 32, 34, 35] compare Pt–Ru and Pt–Os electrodes and show that Os deposits had a better catalytic activity than Ru deposits for methanol oxidation at potentials of 0.6–0.7 V, while Ru is more active for this reaction at potentials lower than 0.6 V. According to these authors, the Ru deposits present excessively higher oxidation states in the potential range of 0.6–0.7 V, which is known to be prejudicial to the catalytic activity of the electrode. Moreover, the Os deposits present a small anodic wave in this potential region (approx. 0.65 V), related to OsO_2 formation. This enhances significantly the catalytic activity of Pt–Os electrodes for methanol oxidation, as well as avoiding the complete formation of Ru oxides in their highest oxidation states in a Pt–Ru–Os ternary electrode [39]. The addition of Os on the Pt single crystal surface has showed an enhancement of the catalytic effect for ethanol oxidation [43].

The present work focuses on ethanol oxidation on Pt alloy catalysts (Pt–Os and Pt–Ru–Os) prepared in an arc-melting furnace. Chronoamperometric measurements were performed with each catalyst to compare their electroactivities to that of Pt alone. Results obtained from the studies of the electrooxidation of ethanol by two spectroscopic methods of in situ FTIRS were discussed in terms of reaction mechanism.

Materials and methods

The polycrystalline Pt-based Ru and Os alloys electrodes were prepared in an arc-melting furnace under argon atmosphere (1.3×10^{-5} bar). The basic atomic compositions of Pt–Ru–Os (70:20:10) and Pt–Os (80:20) were evaluated by energy-dispersive X-ray microanalyses [33, 39].

The electrochemical activity of the materials was examined in 0.2 mol L^{-1} C_2H_5OH+0.5 mol L^{-1} H_2SO_4 solutions by cyclic voltammetry and chronoamperometry in a thermostated three-electrode cell. The electrochemical measurements were performed on a personal computer-controlled VoltaLab Potentiostat PGZ 420 Electrochemical Interface. A reversible hydrogen electrode (RHE) and vitreous carbon were used as the reference and counter electrode, respectively. The electrochemical surface area of the electrodes was obtained from the integration of the hydrogen adsorption/desorption region of the cyclic voltammograms recorded in acid solution (0.5 mol L^{-1} H_2SO_4) at 50 mV s^{-1}.

The spectroelectrochemical investigations were carried out in a Fourier transform infrared (IR) spectrometer Bruker IFS 66v, with the sample compartment modified to allow the beam to be reflected on the electrode surface with an incidence angle of 65°, after passing through the IR window (CaF_2) of a conventional thin-layer spectroelectrochemical cell. The beam path was under vacuum, and a liquid N_2-cooled Hg–Cd–Te detector (Infrared Associates) was used.

Using the single potential alteration infrared reflectance spectroscopy (SPAIRS) technique [15, 17, 19], reflectivities were recorded at 50-mV intervals during the first voltammetric scan at a low sweep rate (1 mV s^{-1}). Each spectrum was the resulted from the coaddition of 128 interferograms. Data acquisition required 20 s, i.e., over approx. 20 mV. Spectra were calculated as $-\Delta A=\Delta R/R=(R_{E2}-R_{E1})/R_{E1}$, where the "reference" spectrum, R_{E1}, was that recorded at

the initial potential at 50 mV vs RHE. Similarly, using the subtractively normalized interfacial Fourier transform infrared reflectance spectroscopy (SNIFTIRS) method [19, 20, 22, 25], reflectivities were obtained at two electrode potentials E_1 and E_2 (the frequency of potential modulation was 25 mHz, and 128 interferograms were collected before the Fourier transform) and coadded 30 times at each potential. The final spectra were normalized as $-\Delta A=\Delta R/R=(R_{E2}-R_{E1})/R_{E1}$. For the SNIFTIRS and SPAIRS calculations, $E_2>E_1$, so that a positive absorption band indicates the consumption of species and a negative absorption band means the production of species. Both techniques allowed the detection of adsorbed species and reaction products at the electrode surface.

Results and discussion

The cyclic voltammogram profile for Pt–Os and Pt–Ru–Os alloy electrodes in acid solution (0.5 mol L^{-1} H_2SO_4) was performed and discussed elsewhere [33]. Briefly, the voltammograms exhibit a similar profile of the Pt electrode (Fig. 1). At 0.7 V vs RHE, a shoulder because of the osmium and/or ruthenium oxides formation is observed. These oxide formation regions extend and overlay the platinum oxide region. The adsorption–desorption hydrogen regions are only due to the contribution of the Pt metal in the catalysts. This evidence allowed the estimation of the true surface area of the different used electrodes.

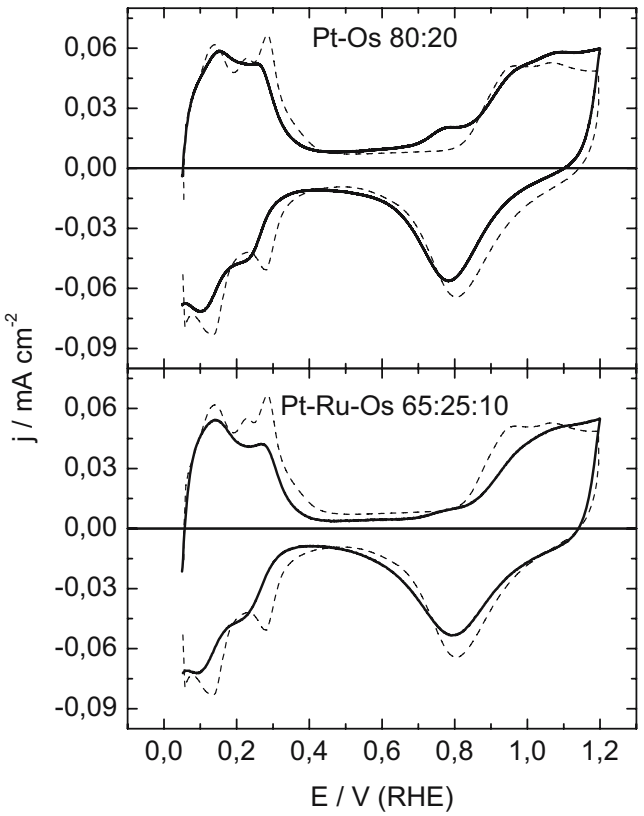

Fig. 1 Voltammetric profiles of Pt, Pt–Os, and Pt–Ru–Os catalysts in 0.5 mol L^{-1} H_2SO_4 solution recorded at a scan rate of 50 mV s^{-1}. *Dashed line*, Pt

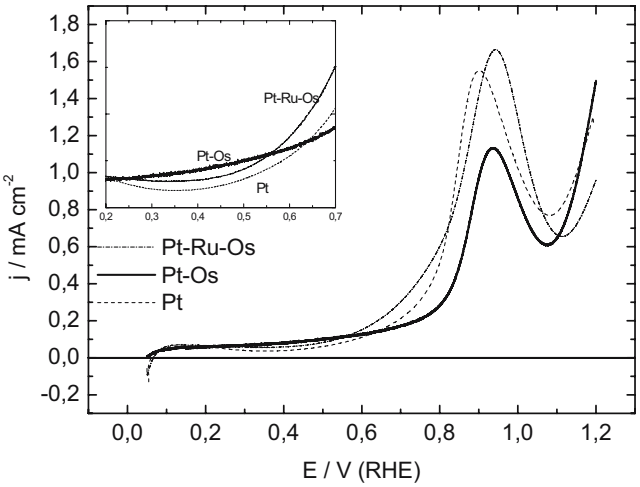

Fig. 2 Anodic sweep curves of Pt, Pt–Os, and Pt–Ru–Os catalysts in 0.2 mol L^{-1} C_2H_5OH+0.5 mol L^{-1} H_2SO_4 solution at a scan rate of 50 mV s^{-1}. *Insert* shows the beginning of ethanol oxidation

The positive scan curves in the presence of ethanol are showed in Fig. 2. Ethanol electrooxidation starts at 300 mV vs RHE, i.e., earlier in the presence of Os and Ru in comparison to a pure Pt catalyst, as can be seen in the inset of Fig. 2. The hydrogen adsorption/desorption regions are clearly suppressed because of the adsorption of organic species. As pointed out by several reports in the literature, the presence of a transition metal such as Os and Ru can promote ethanol oxidation by either an electronic effect in the Pt-based electrode material or by activation of the interfacial water molecule necessary to complete the oxidation of adsorbed CO leading to carbon dioxide or the formation of acetic acid [30–36]. However, at low potentials (from 200 to 400 mV vs RHE), the presence of Os leads to an increase in the catalyst activity by reaching higher current densities, as showed in the detail of Fig. 2. In fact, the introduction of Os and/or Ru leads to an increase in the electroactivity of the binary and ternary electrocatalysts as compared to pure Pt. The synergistic effect obtained with the presence of these elements can be explained by the activation of interfacial water molecules at lower potentials than that observed for pure Pt. According to the bifunctional mechanism, the presence of hydroxyl and/or oxygenated species on Os and Ru sites allows the removal of the poisoning intermediates such as CH_x and CO at lower potentials [30]. Nevertheless, at higher potentials (at approx. 0.9 V), the possible formation of superior Os oxides on the surface prevents further ethanol oxidation, indicating the decrease in the current densities of the Pt–Os

catalyst when comparing to that obtained with pure Pt in the peak potential region.

To evaluate the electrocatalytic performance of the electrodes for ethanol oxidation at low potentials and under long-term operation condition, chronoamperometric measurements were carried out at 400 mV vs RHE. Figure 3 shows the chronoamperograms recorded for different electrode materials whose current values were normalized by the Pt real surface area. At this potential, the current densities reach a steady-state condition for both Pt-based catalysts. Additionally, Pt–Os presents the highest current density. Pt–Ru–Os is much more efficient than pure Pt. These results confirm the same electrocatalytic behavior previously observed in the low-potential region of the cyclic voltammograms in Fig. 1.

To obtain further information about intermediates and reaction products that come from ethanol oxidation on Pt–Os and Pt–Ru–Os catalysts, in situ infrared spectroscopy was performed employing SPAIRS and SNIFTIRS techniques in 0.2 mol L^{-1} C_2H_5OH+0.5 mol L^{-1} H_2SO_4 solution.

Figure 4 shows the SPAIR spectra for Pt–Os and Pt–Ru–Os in the 1,000–3,000 cm^{-1} spectral range and for potentials between 100 and 800 mV vs RHE. These spectra were accumulated at every 50 mV during a cyclic voltammetric experiment runned at 1 mV s^{-1}. The reference reflectivity used for the calculation of $\Delta R/R$ was taken at 50 mV vs RHE. The main bands obtained for the different catalysts are attributed to the presence of linearly adsorbed carbon monoxide, CO_L, CO_2, and acetic acid identified by the bands at 2,044, 2,345, and 1,290, respectively. The band at 1,720 cm^{-1} is attributed to the carbonyl group of both acetaldehyde and acetic acid. Although the main reaction product expected for a complete ethanol oxidation is CO_2, the more intense band (at 1,720 cm^{-1}) observed in the SPAIR spectra is attributed to the presence of both acetic acid and acetaldehyde. The presence of many different bands in the spectra is an evidence that during the ethanol oxidation, several different steps are involved, as already reported elsewhere [25, 44].

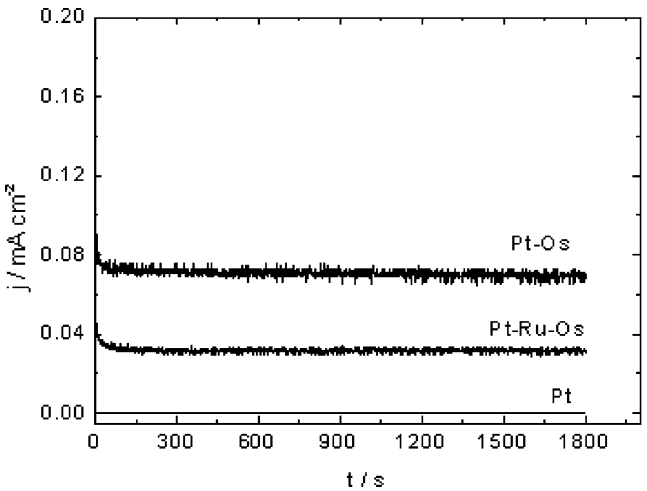

Fig. 3 Potentiostatic oxidation of ethanol on Pt, Pt–Os, and Pt–Ru–Os catalysts during 30 min at 400 mV vs RHE. Solution: 0.2 mol L^{-1} C_2H_5OH+0.5 mol L^{-1} H_2SO_4

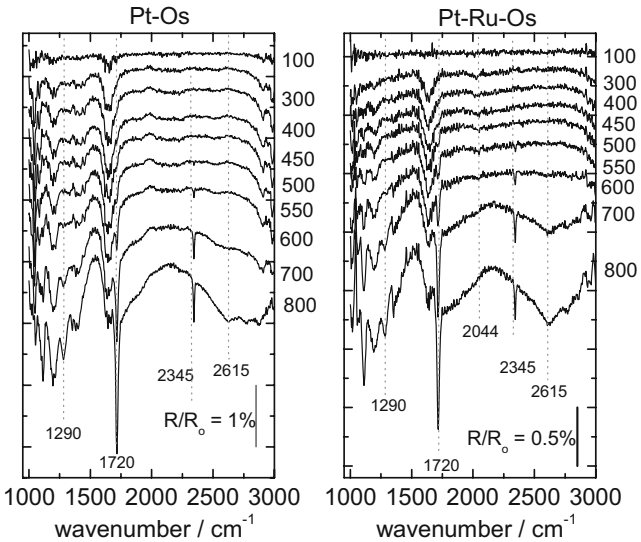

Fig. 4 SPAIR spectra of the species resulting from the oxidation of ethanol in 0.2 mol L^{-1} ethanol+0.5 mol L^{-1} H_2SO_4 on Pt–Os and Pt–Ru–Os at potentials varying from 100 to 800 mV vs RHE. R_{ERef} taken at 50 mV

The band at 1,720 cm^{-1} attributed to the carbonyl, C=O, stretching mode (νCO) is indicative of acetaldehyde and/or acetic acid produced from the ethanol oxidation reaction. The C–O stretching of acetic acid appears at 1,290 cm^{-1} [40, 41, 45]. The presence of this molecule is also evidenced by the simultaneous appearance of a large band at approx. 2,615 cm^{-1} (νCH of CH_3COOH). As evidenced in Fig. 5, the beginning of the production of acetaldehyde (approx. 0.4 V vs RHE) and acetic acid (approx. 0.6 V vs RHE) occurs in different potentials. The bands for acetaldehyde and acetic acid for Pt, Pt–Os, and Pt–Ru–Os catalysts exhibit different intensities. In general, the Pt–Os catalyst displays the most intense relative bands for acetaldehyde and acetic acid as can be seen in Fig. 5. Figure 6 shows the representative curves of the relative intensities of IR bands for CO_2 at the vicinity of the electrode (obtained by SPAIRS) as a function of the electrode potential. It can be observed that the onset potential is the same for all studied catalysts.

The band at 2,044 cm^{-1} (CO_L) is hardly detected by the SPAIRS technique conversely to the SNIFITIRS technique. Figure 7 shows the SNIFTIR spectra recorded in the potential range from 100 to 750 mV at constant potential modulation of 200 mV. The CO_L band appears as a bipolar band at approx. 2,050 cm^{-1}. This band is clearly observed in low potentials, showing that the initial adsorption step of ethanol on both catalysts is a dissociative process.

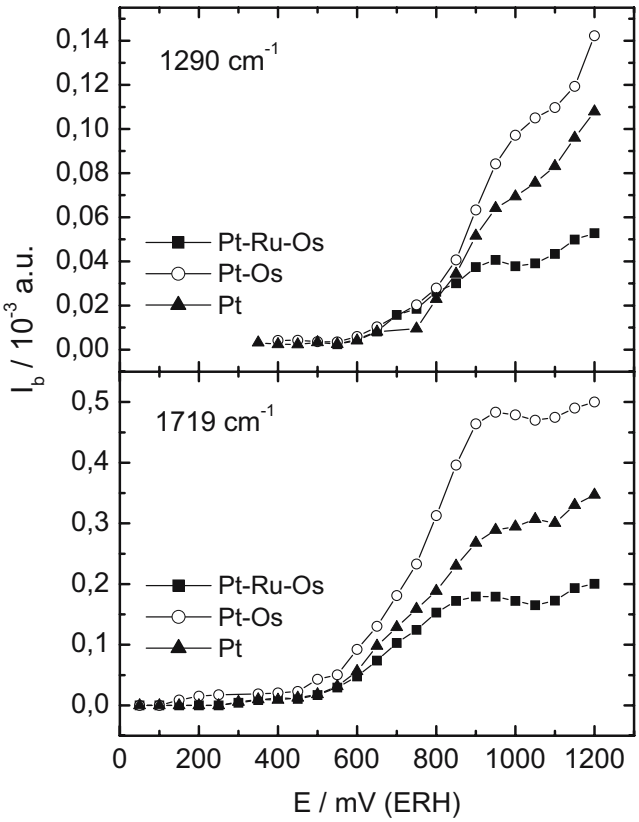

Fig. 5 Comparison between the band intensities of carbonyl (1,720 cm^{-1}) and acetic acid (1,290 cm^{-1}) from SPAIR spectra for ethanol oxidation on Pt, Pt–Os, and Pt–Ru–Os as a function of potential (data obtained from Fig. 4)

It is also observed in Fig. 7, for both catalysts, that the band intensity for CO_L increases, reaches a maximum value around 200–300 mV, and diminishes with the increase in the potential. On pure Pt, the maximum amount of CO_L occurs at higher potentials (more than 400 mV, result not shown in Fig. 6). These results suggest that CO_L exhibits a weaker poisoning effect on Pt–Os and Pt–Ru–Os than on pure Pt. Additionally, the easier facility to oxidize adsorbed CO on Pt-based catalysts provides unequivocally futher evidences of a bifunctional mechanism involving the formation of oxygenated species at lower potentials on osmium and ruthenium atom sites. While adsorbed CO is a poisoning species, it is also a necessary reactive intermediate for futher oxidation to CO_2.

From the various spectroscopic results correlated with the electrochemical measurements, it is possible to infer a parallel pathway mechanism for ethanol electrooxidation as follows:

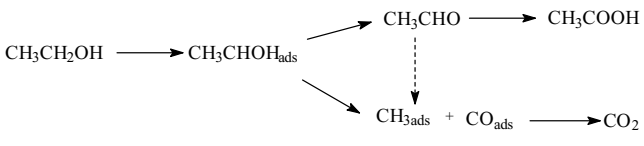

The band at 1,720 cm^{-1} can be interpreted as proceeded from the direct oxidation of ethanol to acetaldehyde and subsequently to acetic acid as suggested by the different potential onsets for the formation of these species (see Fig. 5). The presence of these C_2 molecules suggests that ethanol can react at the Pt surface to produce acetaldehyde. Then, adsorbed oxygenated species on Os and/or Ru sites participate for the formation of acetic acid with a four-electron conversion pathway. Another possible pathway for ethanol oxidation consists of the cleavage of the C–C bond, as CO and CO_2 were determined as the intermediate and reaction product, respectively. The band at 1,636 cm^{-1} is attributed to δ(HOH) of adsorbed water. Indeed, at low potentials (as shown in Fig. 4), adsorbed oxygenated species on Os and/or Ru sites can be used to provide the O atom necessary to transform acetaldehyde and CO into acetic acid and CO_2, respectively, according to the bifunctional mechanism. As can be seen in Fig. 6, CO_2 formation starts at around 500 mV vs RHE for both catalysts; however, Pt–Os electrode presents the most relatively intense bands.

As can be seen in Fig. 7, the adsorbed CO is not more present in the catalyst surface at potentials higher than 600–700 mV. However, from Fig. 6, it can be observed that the CO_2 formation continues in potentials up to 1,200 mV. This is an evidence that acetaldehyde can oxidize to CO_2 at high potentials, as show in the proposed mechanism.

Finally, a band located around 1,385–1,410 cm^{-1} appears at 300 mV vs RHE and increases with the potential. This band can be attributed to OCO stretching mode (ν_sOCO) of the absorbed acetate ions [45]. Maçôas et al. suggested that the γ_{C-H} rocking mode and the CO–COH deformation because of the presence of HCOOH appear in this wave number region [46]. In a previous work, we have determined by liquid chromatography formic acid as a reaction product of acetaldehyde oxidation [33]. However, in this work, there is no direct evidence of formation of formic acid.

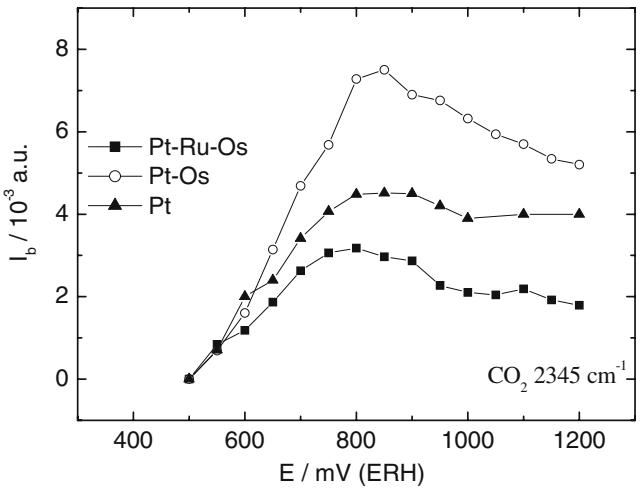

Fig. 6 Comparison between the band intensities of CO_2 (2,345 cm^{-1}) from SPAIR spectra for ethanol oxidation on Pt, Pt–Os, and Pt–Ru–Os as a function of potential (data obtained from Fig. 4)

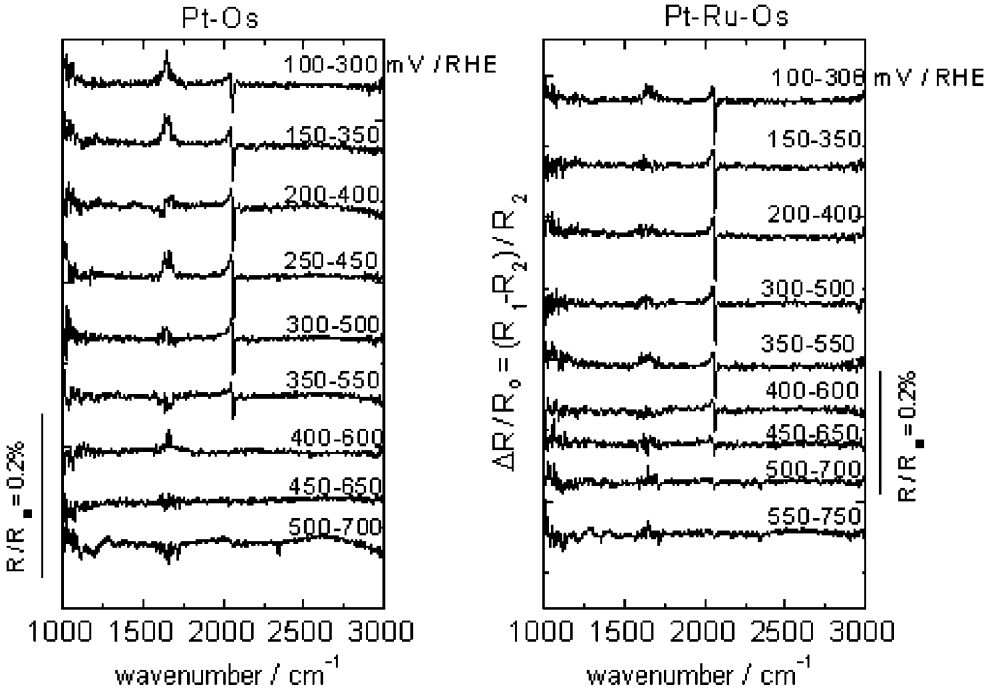

Fig. 7 SNIFTIR spectra of the species resulting from the oxidation of ethanol in 0.2 mol L^{-1} ethanol+0.5 mol L^{-1} H_2SO_4 on Pt–Os and Pt–Ru–Os at various potential modulations from 100 to 750 mV

Conclusions

Pt-based alloy electrocatalysts prepared by an arc-melting furnace process show a catalytic activity toward the ethanol oxidation reaction. Chronoamperometric measurements at 0.4 V vs RHE in the presence of ethanol show, on Pt–Os catalyst, stable current densities twice higher than those obtained with a ternary Pt–Ru–Os catalyst. In all cases, ethanol oxidation starts at lower potentials on Pt-based electrodes than on pure Pt. This indicates also that the presence of the transition metals such as Os and Ru contributes to the activation of interfacial water to form oxygenated species at the neighboring Pt sites necessary for the removal of the adsorbed intermediates. In situ reflectance IR spectroscopy measurements allowed the determination of the intermediates and the final reaction products, confirming that a second transition metal added to Pt favors, by a bifunctional mechanism, the cleavage of the C–C bond and the electrooxidation of strongly adsorbed species like CO to carbon dioxide. SPAIRS and SNFTIRS results support the idea that ethanol oxidation proceeds via a parallel pathway mechanism. On the one hand, adsorbed ethanol is oxidized to acetaldehyde and then to acetic acid. On the other hand, Os and Ru not only promote ethanol oxidation on Pt at low potentials but also increase the current efficiency of CO_2. This catalytic effect can favor the C–C bond cleavage to form CO_{ads} and a methyl group (CH_3).

Acknowledgments This work was mainly conducted under the framework of a collaborative program CAPES/COFECUB under grant no. 498/05/07. D. M. dos Anjos thanks CAPES for the Ph.D. fellowship. G. Tremiliosi-Filho acknowledge FAPESP and CNPq (Brazil) for the financial support.

References

1. Cosmi C, Macchiato M, Mangiamele L, Marmo G, Pietrapertos F, Salvia M (2003) Energy Policy 31:443
2. Wachsmann U, Tolmasquim MT (2003) Renew Energy 28:1029
3. Muhida R, Park M, Dakkak M, Matsuura K, Tsuyosh A, Michira M (2003) Sol Energy Mater Sol Cells 75:697
4. Léger J-M (2001) J Appl Electrochem 31:767
5. Colmati F, Antolini E, Gonzalez ER (2007) J Electrochem Soc 154:B39
6. Vigier F, Coutanceau C, Hahn F, Belgsir EM, Lamy C (2004) J Electroanal Chem 563:81
7. Caillard A, Coutanceau C, Brault P, Mathias J, Léger J-M (2006) J Power Sources 162:66
8. Lamy C, Belgsir EM, Léger J-M (2001) J Appl Electrochem 31:799
9. Maillard F, Gloaguen F, Hahn F, Léger J-M (2002) Fuel Cells 2:143
10. Rousseau S, Coutanceau C, Lamy C, Léger J-M (2006) J Power Sources 158:18
11. Willsau J, Heitbaum J (1985) J Electroanal Chem 27:194
12. Bittins-Cattaneo B, Wilhelm S, Cattano E, Buschmann HW, Vielstich W (1988) Ber Bunsenges Phys Chem 92:1210
13. Iwasita T, Pastor E (1994) Electrochim Acta 39:531
14. Schmiemann U, Muller U, Baltruschat H (1995) Electrochim Acta 40:99

15. Beden B, Lamy C, Bewick A, Kumimatsu K (1981) J Electroanal Chem 121:343
16. Leung L-WH, Weaver MJ (1988) J Electroanal Chem 240:341
17. Beden B, Lamy C (1988) In: Gale RJ (ed) Spectroelectrochemistry, theory and practice (Chapter 5). Plenum, New York, p 189
18. Leung L-WH, Chang S-C, Weaver MJ (1989) J Electroanal Chem 266:317
19. Beden B, Léger J-M, Lamy C (1992) Electrocatalytical oxidation of oxygenated aliphatic organic compounds at noble metal electrodes. In: Bockris JOM, Conway BE, White RE (eds) Modern aspects of electrochemistry, vol. 22. Plenum, New York, p 97
20. Iwasita T, Nart FC (1997) In-situ infrared Fourier transform spectroscopy: a tool to characterize the metal-interface at a molecular level. In: Gerischer H, Tobias CW (eds) Advances in electrochemical science and engineering, vol. 4. Wiley, New York, p 123
21. Kabbabi A, Faure R, Durand R, Beden B, Hahn F, Léger J-L, Lamy C (1998) J Electroanal Chem 444:41
22. Sun S-G (1998) In: Lipkowski J, Ross PhN (eds) Electrocatalysis, frontiers in electrochemistry. Wiley, New York, p 243
23. Iwasita T, Hoster H, John-Anaker A, Lin WF, Vielstich W (2000) Langmuir 16:522
24. Rodriguez JL, Pastor E, Xia XH, Iwasita T (2000) Langmuir 16:5479
25. Iwasita T (2002) Electrochim Acta 47:3663
26. Camara GA, Iwasita T (2005) J Electroanal Chem 578:315
27. Silva-Chong J, Méndez E, Rodriguez JL, Arévalo MC, Pastor E (2002) Electrochim Acta 47:1441
28. Roth C, Martz N, Hahn F, Léger J-M, Lamy C, Fuess H (2002) J Electrochem Soc 149:E433
29. Shin J, Tornquist WJ, Korzeniewski C, Hoaglund CS (1996) Surf Sci 364:122
30. Watanabe M, Motoo S (1975) J Electroanal Chem 60:275
31. Crown A, Moraes IR, Wieckowski A (2001) J Electroanal Chem 500:333
32. Waszczuk P, Lu C-Q, Wieckowski A, Lu C, Rice C, Masel RI (2002) Electrochim Acta 47:3637
33. Kokoh KB, Hahn F, Belgsir EM, Lamy C, de Andrade AR, Olivi O, Motheo AJ, Tremiliosi-Filho G (2004) Electrochim Acta 49:2077
34. Tremiliosi-Filho G, Kim H, Chrzanowski W, Wieckowski A, Grzybowska B, Kulesza P (1999) J Electroanal Chem 467:143
35. Spendelow JS, Lu GQ, Kenis PJA, Wieckowski A (2004) J Electroanal Chem 568:215
36. Roth C, Papworth AJ, Hussain I, Nichols RJ, Schiffrin DJ (2005) J Electroanal Chem 581:79
37. Frelink T, Visscher W, Van Veen JAR (1996) Langmuir 12:3702
38. Lu C, Rice C, Masel MI, Babu PK, Waszczuk P, Kim HS, Oldfield E, Wieckowski A (2002) J Phys Chem B 106:958
39. Liu R, Iddir H, Fan Q, Hou G, Bo A, Ley KL, Smotkin ES, Sung Y-E, Kim H, Thomas S, Wieckowski A (2000) J Phys Chem B 104:3518
40. Souza JPI, Rabelo FJB, de Moraes IR, Nart FC (1997) J Electroanal Chem 420:17
41. Camara GA, de Lima RB, Iwasita T (2005) J Electroanal Chem 585:128
42. Fujiwara N, Friedrich KA, Stimming U (1999) J Electroanal Chem 472:120
43. Pacheco Santos V, Tremiliosi-Filho G (2003) J Electroanal Chem 554:395
44. Léger J-M, Rousseau S, Coutanceau C, Hahn F, Lamy C (2005) Electrochim Acta 50:5118
45. Shao MH, Adzic RR (2005) Electrochim Acta 50:2415
46. Maçôas EMS, Lundell J, Pettersson M, Khriachtchev L, Fausto R, Räsänen M (2003) J Mol Spectrosc 219:70